Redox Biology 47 (2021) 102169

Contents lists available at ScienceDirect

Redox Biology

journal homepage: www.elsevier.com/locate/redox

Sulfide-quinone oxidoreductase is required for cysteine synthesis and indispensable to mitochondrial health

Xi Zhang [a], Yuping Xin [a], Zhigang Chen [a], Yongzhen Xia [a], Luying Xun [a,b,**], Huaiwei Liu [a,*]

[a] State Key Laboratory of Microbial Technology, Shandong University, Qingdao, 266237, PR China
[b] Department of Chemistry, School of Molecular Biosciences, Washington State University, Pullman, WA, 99164-4630, USA

ARTICLE INFO

Keywords:
Mitochondria health
Reactive sulfur species
Sqr
Cysteine biosynthesis
Hydrogen sulfide
Schizosaccharomyces pombe

ABSTRACT

Mitochondrial dysfunction is related to common age-related disorders, including neurodegenerative diseases, metabolic syndrome, and carcinogenesis. Therefore, maintaining the functionality and integrity of mitochondria is important for human health. Herein, we found that sulfide:quinone oxidoreductase (Sqr), which oxidizes hydrogen sulfide to reactive sulfur species (RSS), was indispensable to mitochondria health in the eukaryotic model microorganism *Schizosaccharomyces pombe*. Sqr knock-out led to morphological changes and functional deficiencies of mitochondria and apoptosis in *S. pombe*. The Sqr knock-out strain displayed the same phenotypes as the cysteine-synthesis-deficient strain, and cysteine addition complemented the effects caused by Sqr knock-out. In *S. pombe*, Sqr was the main RSS producer in mitochondria, and RSS instead of H_2S was used by cysteine synthase to synthesize cysteine. This finding rewrites the cysteine biosynthesis route in *S. pombe* and may also in other eukaryotes and prokaryotes, and highlights the importance of cysteine and RSS in maintaining mitochondrial health.

1. Introduction

Mitochondria exert a broad range of vital functions in eukaryotic cells. They produce over 80% of cellular energy via oxidative phosphorylation [1]. As a hectic distribution station of metabolites, they play a key role in cellular central metabolism including the tricarboxylic acid cycle (TCA cycle), fatty acids degradation, and amino acids biosynthesis, as well as the heme production, iron-sulfur cluster biogenesis, and calcium homeostasis [2]. Therefore, maintaining the functionality and integrity of mitochondria is important for human health. Dysfunction of mitochondria is observed in common age-related disorders, including neurodegenerative diseases, metabolic syndrome, and carcinogenesis [3–6].

Sulfane sulfur-containing species are a subset of RSS (reactive sulfur species), which includes inorganic polysulfide (HS_nH, $n \geq 2$), organic polysulfide (RS_nH, $n \geq 2$), and polysulfane (RS_nR, $n \geq 2$) [7,8]. RSS plays critical functions in the cell, such as signaling, redox homeostasis maintenance, and metabolic regulation [9–11]. A few RSS producing enzymes have been identified [12]. Cystathionine beta-synthase (Cbs) and cystathionine gamma-lyase (Cse) mainly locate in cytoplasm; 3-mercaptopyruvate sulfurtransferase (3-Mst) and cysteinyl-tRNA synthetase 2 (Crs2) mainly locate in mitochondria. These four enzymes use cysteine or its oxidized form cystine as a precursor to generate RSS. Differently, sulfide:quinone oxidoreductase (Sqr) uses an inorganic substrate, hydrogen sulfide (H_2S), to generate RSS in mitochondria [13–15]. Excessive RSS is oxidized to sulfite by persulfide dioxygenase (Pdo, also named as ETHE1) in mitochondrial matrix in mammalian cells [16,17]. Recently, it is observed that impairing RSS biogenesis by knocking down Crs2 leads to obvious mitochondrial dysfunction, intimating that RSS metabolism is highly related with mitochondrial health [18]. Sqr is a specific RSS producer in the mitochondria of many eukaryotes including human [19]. However, the role of Sqr in maintaining mitochondiral health has not been reported.

There are several challenges for studying Sqr directly in mammalian cells. First, knocking-out Sqr is lethal to mammalian cell, and currently no specific Sqr inhibiting compound is available. Second, even Sqr is successfully knocked out/down, the possibility that cytoplasmic RSS transports into mitochondria for functional complementation cannot be excluded. Third, in the presence of Pdo, the effect of Sqr overexpression will be compromised. The fission yeast *Schizosaccharomyces pombe* has

* Corresponding author. 72 Binhai Road, Qingdao, 266237, PR China.
** Corresponding author. Smith Center 519, Washington State University, Pullman, WA, 99164-7520, USA.
E-mail addresses: luying_xun@vetmed.wsu.edu (L. Xun), liuhuaiwei@sdu.edu.cn (H. Liu).

https://doi.org/10.1016/j.redox.2021.102169
Received 19 August 2021; Received in revised form 9 October 2021; Accepted 14 October 2021
Available online 15 October 2021

long been used as a model for studying eukaryotic cells [20,21]. In terms of RSS metabolism, *S. pombe* does not contain genes encoding Cbs, Cse, Crs2, or Pdo. It only has mitochondrial enzymes Sqr and 3-Mst, providing an ideal platform for studying the Sqr's role in maintaining mitochondrial health [22]. Herein, we revealed that Sqr is the main RSS generating enzyme in *S. pombe* mitochondria. The Sqr knock-out strain (*Δsqr*) displayed low cell viability and signs of early apoptosis. The mitochondrial integrity and functionality were impaired in *Δsqr*. Further investigation indicated that the cysteine *de novo* biosynthesis process was hampered by Sqr knock-out.

2. Materials and methods

2.1. Strains and materials

S. pombe HL6381 and its derivatives, *E. coli* strains used for plasmid construction and protein expression, plasmids constructed in this study are all listed in Supplementary Table S1. For routine growth, *S. pombe* strains were cultivated in yeast extract medium (YES), Edinburgh minimal medium (EMM), or synthetic dropout medium (SD). Specific supplements were added when required as mentioned in main text. The cultivation was performed at 30 °C. For hypoxic cultivation, *S. pombe* was cultivated in YES medium at 30 °C with shaking (220 rpm). The log-phase cells were harvested and then diluted to OD_{600} of 0.02 in the anaerobic bottle. Before inoculation, the YES medium in the anaerobic bottle was deoxygenated by blowing argon gas into it (20 min). At each sampling time, cells were collected by using the syringe.

E. coli strains were cultured in lysogeny broth (LB) medium at 37 °C. Sodium hydrosulfide (NaHS), cysteine, reduced glutathione (GSH), and thiosulfate were purchased from Sigma-Aldrich (Saint Louis, MO). Dimethyl trisulfide (MeSSSMe) and S_8 were purchased from TCI Company (Shanghai, China). HS_nH was prepared following the protocol of Luebke et al. [23].

GSSH was prepared following the protocol of Liu et al. [24]. Briefly, the elemental sulfur (S_8) was dissolved in acetone to make a saturated sulfur solution (~17 mM). GSH was dissolved in distilled water (17 mM). The two solutions were mixed at 1:1 ratio (volume) in 100 mM Kpi buffer (pH 7.4) to make GSSH. The cyanide derivatization method was used to determine the GSSH concentration, which was 4.05 ± 0.19 mM. The methylene blue method was used to determine how much HS^- in it and only 54.5 ± 19.2 μM was detected. Potential disturbance caused by such low percentage of HS^- in GSSH solution can be neglected.

2.2. H_2S and RSS detection

H_2S production of *S. pombe* strains was detected using the lead acetate assay method [25]. Briefly, a lead-acetate paper strip was affixed to the inner wall of a 15-ml glass tube containing 3 ml of the strain culture. When H_2S was produced and evaporated into the gas phase, it reacted with Pb(II) in the paper strip to form PbS black precipitate. To quantify the intracellular H_2S, log-phase cells were collected and re-suspended in a reaction buffer (50 mM Tris-HCl, pH 9.5, 1% Triton X-100, 50 μM DTPA). To disrupt cells, they were incubated at 95 °C for 15 min. The HS^- in cell lysate was labeled with monobromobimane (mBBr) and quantified by HPLC following a previously reported protocol [26]. RSS detection was performed using a HPLC-based method reported previously [27]. Briefly, *S. pombe* cells were collected and re-suspended in a reaction buffer (50 mM Tris-HCl, pH 9.5, 1% Triton X-100, 50 μM DTPA, 50 mM sulfite), and incubated at 95 °C for 10 min to convert intracellular RSS to thiosulfate. The thiosulfate was labeled with mBBr and quantified by HPLC.

2.3. Protein expression and purification

The gene encoding Cys11 was amplified from genomic DNA of *S. pombe* YHL6381. For Cys11 expression and purification in *E. coli*, a maltose binding protein (MBP) tag was fused to its N-terminus. The expression plasmid pMal-*cys11* was constructed and introduced into *E. coli* BL21(DE3) and the strain was incubated in LB medium containing ampicillin (100 μg/ml). When OD_{600} reached 0.6, 0.3 mM isopropyl β-D-1-thiogalactopyranoside (IPTG) was added and the temperature was decreased to 25 °C. The cultivation was further continued for 22 h. Cells were harvested by centrifugation and then re-suspended in CB buffer (20 mM Tris-HCl, 0.2 M NaCl, 1 mM EDTA, pH 7.4). Cell disruption was performed using a Pressure Cell Homogeniser (SPCH-18) at 4 °C. Cell lysate was centrifuged to remove the debris and Cys11 was purified by using an amylose resin column.

2.4. Enzymatic activity assay

To obtain the Cys11 crude enzyme, *S. pombe* cells were suspended in a lysis buffer (50 mM PBS, pH7.4) containing a protease inhibitor cocktail (Sigma-Aldrich, P8340), and disrupted using the pressure cell homogenizer (SPCH-18). The cell lysate was centrifuged at 12,500 g for 15 min to remove cell debris and the obtained supernatant was used as crude Cys11.

Cys11 activity assay was carried out as described previously [28]. Briefly, 0.1 ml reaction buffer (50 mM PBS buffer, pH 7.4) contained 2 mg/ml crude Cys11 or 0.1 mg/ml purified Cys11, 100 μM pyridoxal phosphate, 1.0 mM–2.0 mM OAS, 1.0–5.0 mM NaSH, GSSH, or $Na_2S_2O_3$. The reaction was conducted at 30 °C for 5 min and the produced L-cysteine was quantified using a previously reported method [29].

For kinetics assay, 0.1 ml reaction buffer (10 mM PBS, pH 7.4) contained 0.1 mg/ml purified Cys11, 100 μM pyridoxal 5-phosphate (PLP), and 1 mM O-acetyl-L-serine (OAS). NaSH, GSSH or $Na_2S_2O_3$ was added with varied concentrations as mentioned in main text. The reaction was conducted at 30 °C for 5 min. For the reaction using NaSH as a substrate, the decrease of H_2S was determined by monitoring the formation of methylene blue in absorbance at 670 nm. For the reaction using thiosulfate as a substrate, the remaining thiosulfate was labeled with mBBr and quantified by HPLC [26]. For the reaction using GSSH as a substrate, the reaction solution was mixed with 0.5 mM tris-(2-carboxyethyl)-phosphine (TCEP), and the released cysteine was labeled with mBBr and quantified by HPLC [26]. All kinetic parameters were determined using the Michaelis-Menten equation (non-linear regression) embedded in Graphpad prism software.

2.5. qRT-PCR analysis

S. pombe cells were cultivated to OD_{600} of 0.8–1.5. The total RNA was extracted using an E.Z.N.A. Yeast RNA kit (Omega, R6870) following the manufacturer's protocol. The first-strand cDNA synthesis was acquired from 500 ng of total RNA by using the Prime Script RT reagent kit with genomic DNA eraser (TaKaRa, RR047A). The SYBR Premix Ex Taq II kit (TaKaRa, DRR081A) was used for qRT-PCR analysis, and the reactions were run in a Light Cycler 480 II sequence detection system (Roche). All data were normalized using *act1* (SPBC32H8.12c) mRNA as the reference gene. Primers used for qRT-PCR analysis are listed in Supplementary Table S2.

2.6. mtDNA number analysis

Quantitative PCR (qPCR) method was used to analyze the relative number of mtDNA. Genomic DNA (gDNA) of *S. pombe* cells was extracted using an E.Z.N.A.TM Yeast DNA kit (Omega D3370). A total of 100 ng of genomic DNA was used as the template. The *cox1* and *act1* genes were used to represent mitochondrial DNA and nuclear DNA, respectively. Their cycle threshold (CT) values were obtained from three parallels, and the interpolation of CT_{COX1} and CT_{ACT1} was calculated to get the ΔCT, $2^{\Delta CT}$ was used to represent the relative number of mtDNA.

2.7. Apoptosis analysis

The Annexin V-FITC Apoptosis Detection Kit (Beyotime Biotechnology, C1062S) was used to monitor the externalization of phosphatidylserine and membrane permeability of *S. pombe* cells as described previously [30,31]. After a 24 h growth in YES medium, 1×10^6 *S. pombe* cells were collected and washed twice with sorbitol buffer (1.4 Msorbitol, 40 mM HEPES, 1.5 mM $MgCl_2$, pH 6.5). To prepare protoplasts, the cells were gently agitated in 1 ml sorbitol buffer containing 10 mg/ml lysing enzymes (Sigma-Aldrich, L1412). After a 1–3 h incubation at 30 °C, cell pellets were washed with 200 μl Annexin V-FITC binding buffer, then re-suspended in 210 μl Annexin V-FITC binding buffer containing 5 μl of Annexin V-FITC and 10 μl of propidium iodine (PI), and incubated at room temperature in the dark for 20 min. The flow cytometer (BD Accuri™ C6) was used to assess Annexin V-FITC and PI staining.

2.8. Survival rate analysis

S. pombe strains were cultivated in YES or EMM medium. At each sampling time, the cells were collected, diluted, and spread on YES medium agar plates. After an incubation at 30 °C for 2 days, the numbers of colonies (CFU) on each plate were counted. The survival rate was determined by calculating the ratio of *Δhmt2* CFU to wt CFU.

2.9. Cell cycle analysis

The classic PI staining method was used to analyze cell cycles of *S. pombe* cells as previously reported [32]. Briefly, log-phase cells were grown to OD_{600} of 0.8–1.0, then harvested and washed two times, and diluted to OD_{600} of 0.1 in EMM medium. 1×10^6 cells were undergone cell wall digestion, and then were fixed in 70% ice cold ethanol. 500 μl PI staining solution was added into the samples. The mixture was incubated at 37 °C for 0.5 h in the dark. For detection, the signals of 50,000 cells were collected by a flow cytometer (BD Accuri™ C6). FlowJo v10.2 software was used for analysis.

2.10. Mitochondrial membrane potential analysis

The fluorescent probe JC-1 assay kit (Beyotime Biotechnology, C2006) was used to evaluate mitochondrial membrane potential. *S. pombe* cells were harvested, washed twice, and suspended in JC-1 work buffer, and then loaded with JC-1 probe following the manufacturer's instruction. The mean fluorescence intensities of monomeric JC-1 (FL1) and aggregated JC-1 (FL2) were measured by a flow cytometer (BD Accuri™ C6). At least 50,000 cells per sample were analyzed. The ratio of FL2 to FL1 fluorescence intensity was calculated with CFlow software (BD Biosciences). Carbonyl cyanide 3-chlorophenyl hydrazone (cccp) treated wt cells were used as the control.

2.11. ROS analysis

Cellular ROS was measured using the DCFH-DA probe (Beyotime Biotechnology S0033S). *S. pombe* strains were cultivated in YES or EMM medium at 30 °C with shaking (220 rpm). At each sampling point, cells were collected by centrifugation (4000 *g*, 5 min), washed twice with 50 mM PBS buffer (pH 7.4), and diluted to OD_{600} of 1.0 in PBS buffer containing 10 μM DCFH-DA. The cell suspensions were incubated at 30 °C for 20 min in the dark, and then were washed three times to remove the extra DCFH-DA. The fluorescence of the cells was measured using a flow cytometer (BD Accuri™ C6). At least 10,000 cells per sample were analyzed. Since Rosup (Beyotime Biotechnology S0033S) treated wt cells increased its ROS level, they were used as the positive control.

2.12. Oxygen consumption analysis

S. pombe strains were grown in YES medium to OD_{600} of 0.8–1.0, and then harvested and washed two times with 50 mM PBS buffer (pH 7.4). OD_{600} was adjusted to 5 in PBS buffer. 1% glucose (w/v) was added. An Orion RDO meter was used to monitor change of O_2 concentration in the cell suspension.

2.13. Mitochondria morphology observation

The green fluorescent protein (GFP) was fused with an N-terminus leading peptide (MFMNSMLRVSRQRAAVRSTVSLYRGFVSASIRR) to locate it into mitochondria inner membrane. The fused GFP (mito-GFP) was ligated into pJK148 plasmid, after the *TEF1* promoter. This plasmid was linearized by *NruI* digestion, and then integrated into the chromosomal *leu1-32* site of *S. pombe* strains. The laser confocal microscope LMS900 was used to observe mitochondrial morphology.

2.14. LC-ESI-MS analysis

The purified Cys11 (0.1 mg/mL) was mixed with PLP (100 μM), OAS (1 mM) and 1 mM GSSH or thiosulfate in the reaction buffer (10 mM PBS, pH 7.4). The reaction was conducted at 30 °C for 5 min. Then, the solution was subjected to LC-ESI-MS analysis (Ultimate 3000, Burker impact HD) following a reported protocol [26]. For detection of the produced L-cysteine, TCEP (0.5 mM) was added to break the disulfide bond. The released cysteine was derivatized with mBBr and then subjected to LC-ESI-MS analysis.

2.15. Transcriptomic analysis

S. pombe strains were firstly cultivated in YES medium for 12 h, and then transferred into EMM medium for another 12 h's cultivation. Cells were harvested for the omics analysis, which were performed at Shanghai Applied Protein Technology Co., Ltd (Shanghai, China). For transcriptomic analysis, total RNA was extracted. Magnetic beads with Oligo (dT) were used to enrich mRNA and fragmentation buffer was added to randomly interrupt the mRNA. The first strand of cDNA was obtained with six-base random primers and the second strand of cDNA was synthesized by adding buffer, dNTPs and DNA polymerase I. Double-stranded cDNA was purified with AMPure XP andthen A-tailing and sequencing adapters were connected. The AMPure XP beads were used for fragment size selection and PCR enrichment was perform to obtain the final cDNA library. The library was sequenced on Illumina NovaSeq 6000 platform. The clean data were obtained from raw data by removing reads containing adapter, poly-N and low quality reads. The clean reads were aligned with the Ensemble genome of ASM294v2 by using HISAT2. The feature Counts software was used to calculate the FPKM value of each gene expression in each sample. Genes with a p-vale$<$0.05 and fold change$>$2 were considered as significantly differentially expressed.

2.16. Targeted metabolomics analysis

For targeted metabolomics analysis, cells were harvested and quickly frozen in liquid nitrogen. After grinding with liquid nitrogen, 60 mg cells were mixed with 1 ml methanol acetonitrile aqueous solution (2:2:1, v/v) and vortexed for 60 s. Cells were disrupted using the ultra-sound method. The broken cells were placed at −20 °C for 1 h and then centrifuged at 14,000g for 20 min at 4 °C. The obtained supernatant was subjected to freeze-dry and then LC-MS analysis. The Waters I-class ultra-performance liquid chromatography was used and the mobile phase A was an aqueous solution containing 25 mM ammonium acetate and 25 mM ammonia (pH, 9.75). Mobile phase B was acetonitrile. Protein sample was placed in a 4 °C auto sampler, and the column temperature was set to 40 °C. The flow rate was 0.3 ml/min, and the

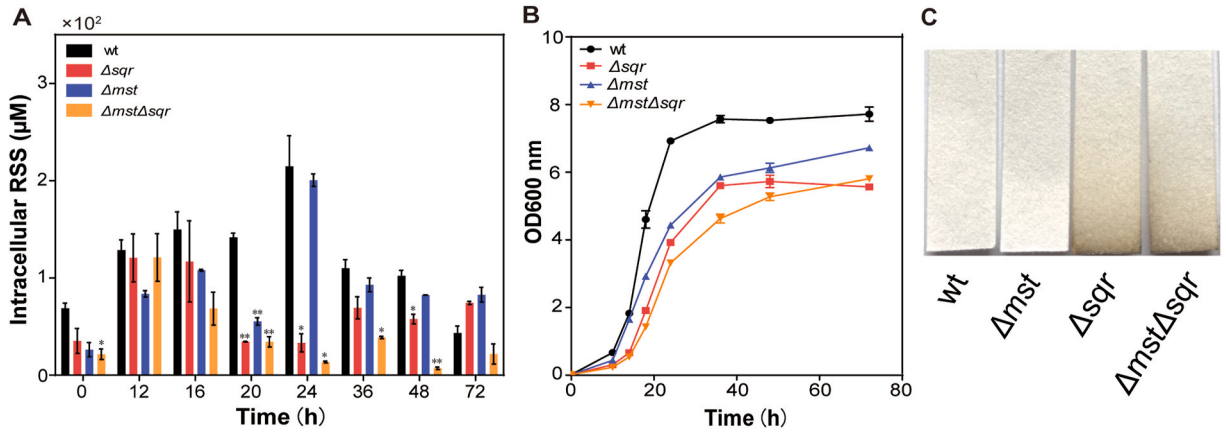

Fig. 1. Growth, intracellular RSS production, and H_2S release of *S. pombe*. A) Intracellular RSS production of the *S. pombe* wt and mutant strains when cultivated in YES medium. B) Growth performance in YES medium. C) Released H_2S from the culture were colorized by lead acetate papers. Data were from three independent experiments and showed as average ± SD.

injection volume was 2 μl. The liquid phase gradient was set as: 0–1 min, phase B at 95%; 1–14 min, B linearly changing from 95% to 65%; 14–16 min, B linearly changing from 65% to 40%; 16–18 min, B at 40%; 18–18.1 min, B linearly changing from 40% to 95%; 18.1–23 min, B at 95%. In the sample cohort, one QC sample was set every six experimental repeats to detect and evaluate the stability and repeatability of the system.

The AB 5500 QqQ mass spectrometer (AB SCIEX, Framingham, MA) was used for mass spectrometry analysis. The ESI source conditions were as: sheath gas temperature, 350 °C; dry gas temperature, 350 °C; sheath gas flow, 11 l/min; dry gas flow, 10 l/min; capillary voltage was 4000 V for positive mode and −3500 V for negative mode; nozzle voltage, 500 V; and nebulizer pressure, 30 psi. Monitor was in MRM mode and the dwell time of each MRM transition was 3 ms, and the total cycle time was 1.263 s. MRM analyzer (R) was used to extract the original MRM data of 200 metabolites to obtain the peak area of each metabolite. Metabolites with p-value<0.05 and fold change>1.5 were considered as at significantly different levels.

2.17. Statistical analysis

Transcriptomics analysis was performed with three parallel biological samples and targeted metabolomics analysis was performed with six parallel biological samples. The data have been deposited in https://www.biosino.org/node/with ID: OEP002326. Other analysis were performed with ≥2 parallel biological samples and repeated ≥2 times. Data are presented as mean ± S.D.

3. Results

3.1. Sqr is the main producer of intracellular RSS in S. pombe

The genes encoding Sqr and 3-Mst are denoted as *hmt2* and *tum1* in *S. pombe* (www.pombase.org). For description convenience, we refer

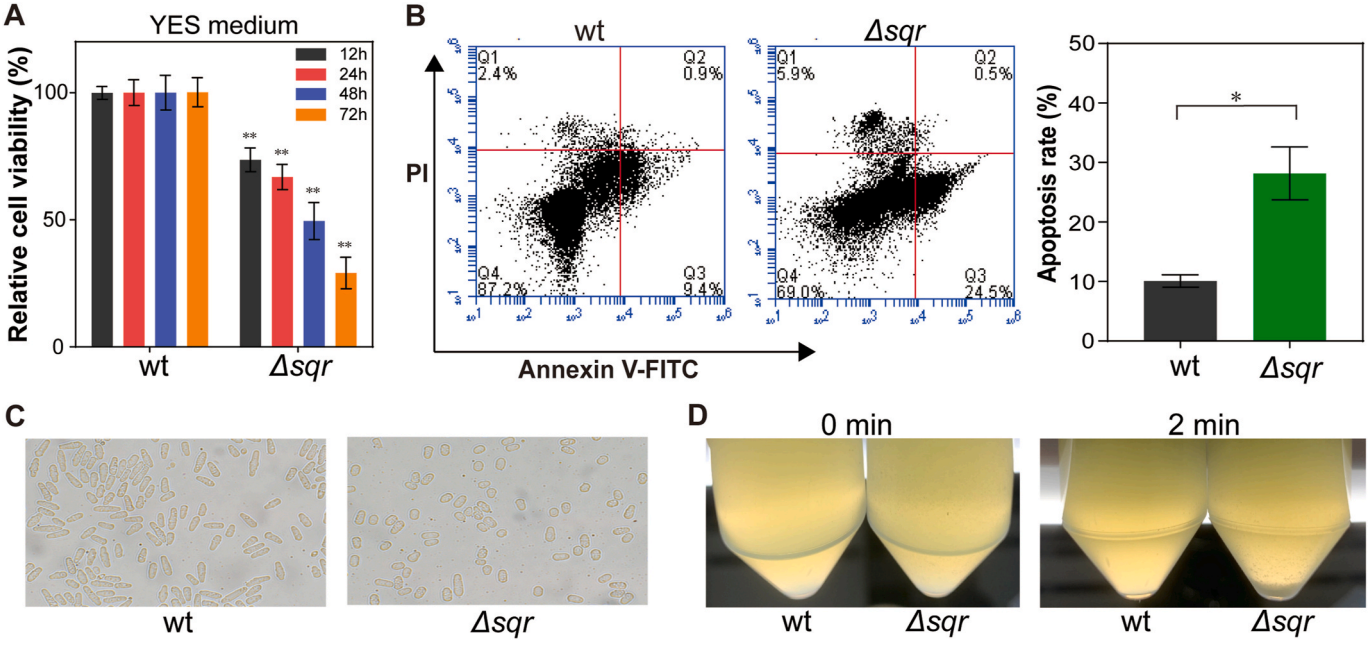

Fig. 2. Sqr knock-out resulted in physiological changes in *S. pombe*. A) The *Δsqr* strain showed reduced cell viability compared to the wt strain when cultivated in YES medium. B) Apoptosis analysis demonstrated that there were more cells of early apoptosis in *Δsqr* culture than that in wt culture (Q3, 24.5% vs 9.4%). C) The *Δsqr* and wt strains showed different morphology. D) The *Δsqr* cells quickly precipitated down in 2 min. Data were from three independent experiments and presented as average ± SD. T-tests were performed to calculate the p-values, and asterisks indicate statistically significant difference (*$p < 0.05$, **$p < 0.01$).

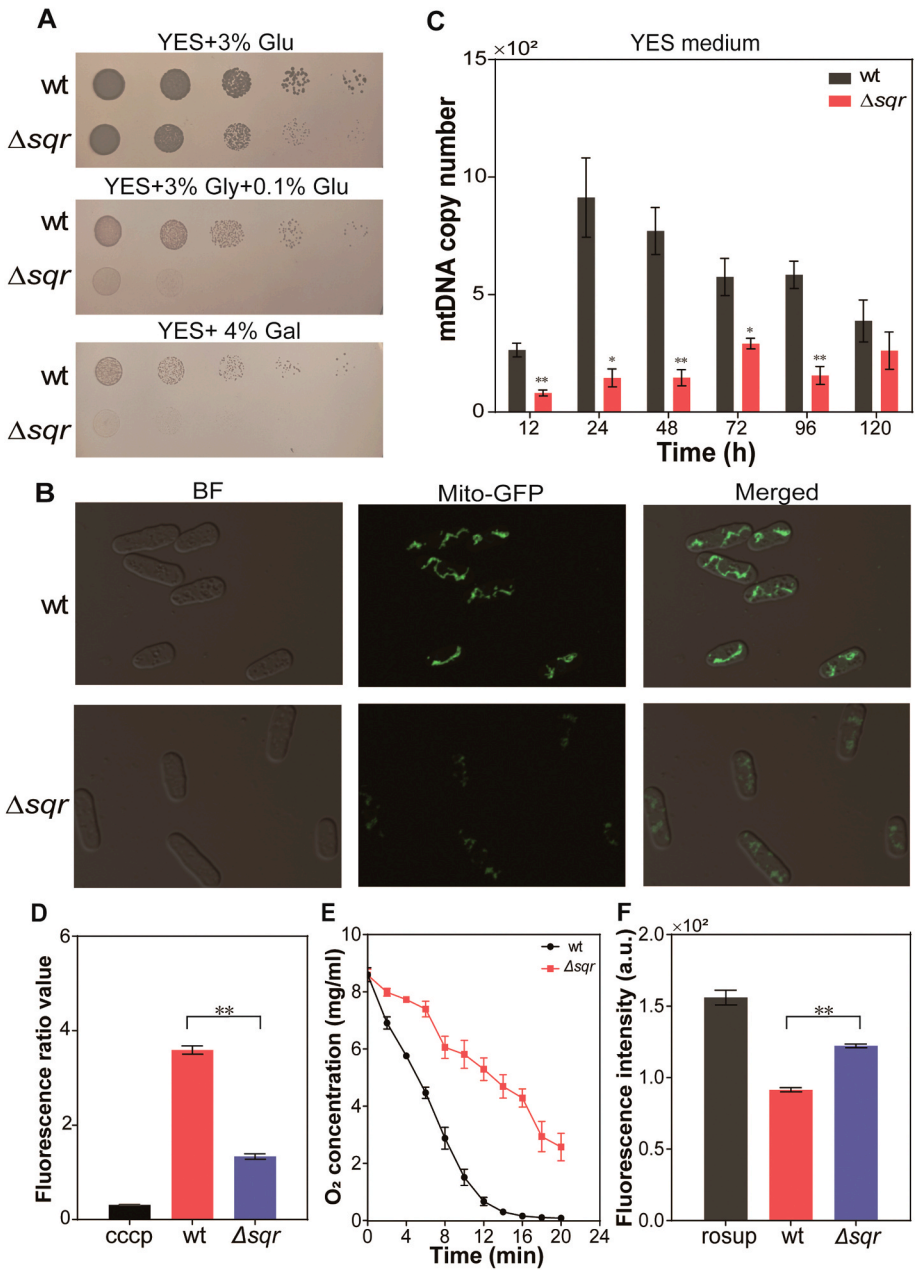

Fig. 3. Sqr knock-out impaired mitochondrial health in *S. pombe*. A) The *Δsqr* and wt strains were cultivated with glucose (Glu, fermentable carbon source), galactose (Gal), or glycerol (Gly). The latter two are none-fermentable carbon sources for *S. pombe*. B) Mitochondrial morphology analysis of *S. pombe* strains. The strains containing mito-GFP were cultivated in YES medium to log phase. Images were captured with the laser confocal microscope LMS900. C) MtDNA analysis of wt and *Δsqr* strains. D) Mitochondrial membrane potential analysis of the wt and *Δsqr* strains. Wt cells treated with cccp (a potent mitochondrial uncoupling agent) were used as the control. E) Oxygen consumption analysis of the wt and *Δsqr* strains with or without glucose addition. F) Analysis of intracellular ROS of the wt and *Δsqr* strains. Wt cells treated with rosup (a potent ROS increasing agent) were used as the control. Data were from three independent experiments and presented as average ± SD. T-tests were performed to calculate the p-values, and asterisks indicate statistically significant difference (*p < 0.05, **p < 0.01).

them as *sqr* and *mst* in this paper. Knocking out them in *S. pombe*y HL6381 led to three mutants: *Δsqr*, *Δmst*, and *ΔsqrΔmst*. Compared to the parent yHL6381 wild type (wt) strain, the *Δsqr* strain showed obviously lower level of intracellular RSS when cultured in YES medium, especially at late-log and stationary phases (20 h–48 h) (Fig. 1A). The *Δmst* strain also displayed decreased level of intracellular RSS, but the decreasing degree was lower than that of *Δsqr*, and RSS decrease only happened at log-phase (before 24 h). The *ΔsqrΔmst* double mutant strain showed similar RSS level as the *Δsqr* strain. These results indicated that in respect of RSS production, Sqr is more important than 3-Mst in *S. pombe*. All the mutants exhibited impaired growth with *Δsqr* and *ΔsqrΔmst* more obviously than *Δmst* (Fig. 1B). Wt and *Δmst* cultures did not release gaseous hydrogen sulfide (H_2S) out, whereas *Δsqr* and *ΔsqrΔmst* cultures did (Fig. 1C), indicating that SQR can oxidize self-produced H_2S in the cell.

The unreleased intracellular H_2S (mostly exists as HS^-) in wt and *Δsqr* cells was quantified. The wt cells contained 15.3 ± 4.9 μM and the *Δsqr* cells contained 51.7 ± 6.7 μM of HS^-, the ratio of wt/*Δsqr* was 0.30. These results further confirmed that SQR is the oxidizer of intracellular H_2S.

3.2. *Sqr knock-out led to various physiological changes including early apoptosis*

We analyzed viability of the *Δsqr* strain that was cultivated in YES medium. The *Δsqr* strain displayed constantly lower viability compared with the wt strain (Fig. 2A). We then used the apoptosis detection kit Annexin V-FITC and PI to stain both wt and *Δsqr* cells, and observed that 24.5% of *Δsqr* cells was stained with Annexin V-FITC but not with PI (AnnexinV-FITC+, PI-, lower right quadrant, Fig. 2B); whereas, the corresponding percentage of wt cells was 9.4%, indicating that there were more early-apoptotic cells in *Δsqr* culture than in wt culture. In addition to these physiological changes, *Δsqr* cells displayed a different morphology with a round shape (Fig. 2C). The *Δsqr* cells also formed aggregates, which easily precipitated down (Fig. 2D).

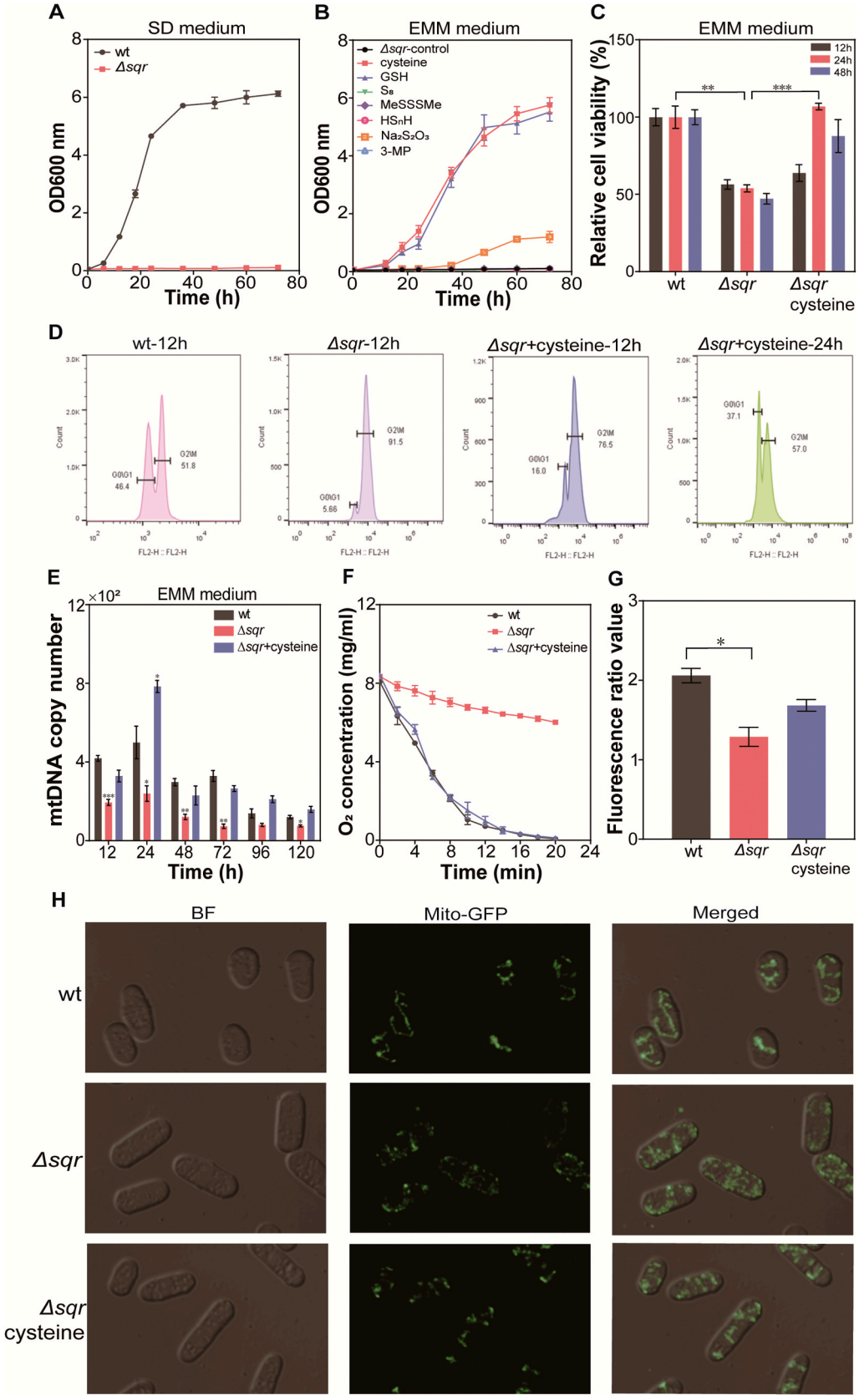

Fig. 4. Cysteine complemented the effects caused by Sqr knock-out. A) The *Δsqr* strain lost the ability of growing in cysteine-deficient medium (SD or EMM). B) Cysteine and GSH (0.2 mM) restored the growth of *Δsqr* in EMM medium. $Na_2S_2O_3$ (0.1 mM) partially restored the growth while other RSS (0.1 mM) did not. C) Cell viability of *Δsqr* was lower than that of wt, but it was restored by cysteine treatment. D-H) Cell cycle, mtDNA number, oxygen consumption, mitochondrial membrane potential, and mitochondrial morphology analysis of the wt, *Δsqr*, and cysteine-treated *Δsqr* strains, 500 μM cysteine was used to treat *Δsqr*. Data were from three independent experiments and presented as average ± SD. T-tests were performed to calculate the p-values, and asterisks indicate statistically significant difference (*$p < 0.05$, **$p < 0.01$, ***$p < 0.001$).

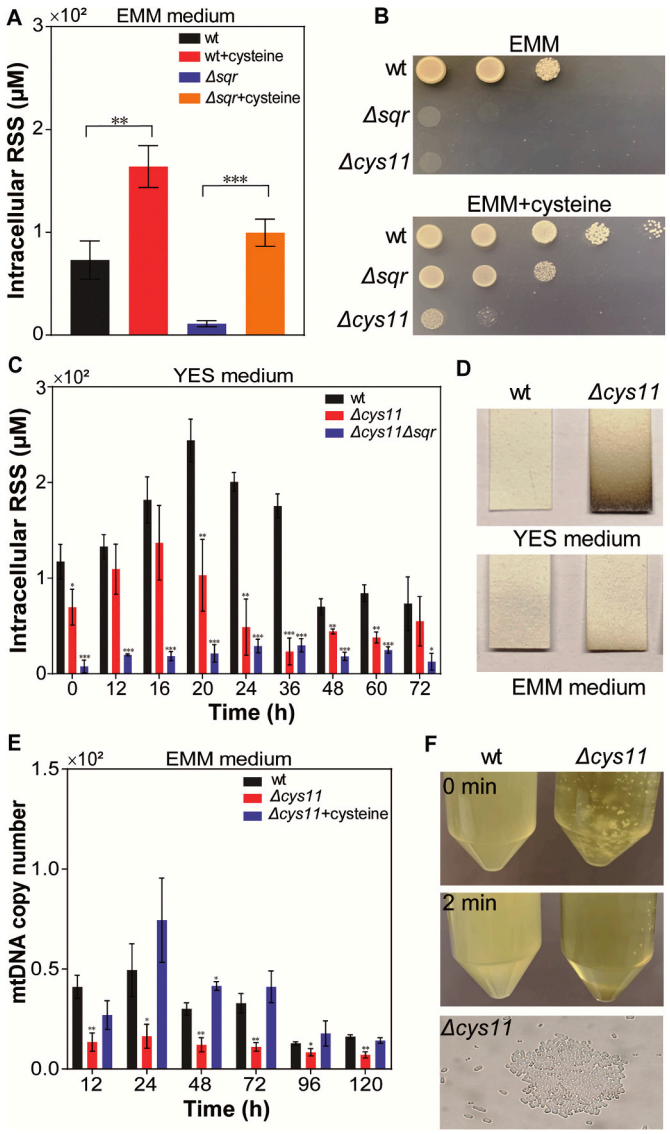

Fig. 5. Sqr was involved in cysteine biosynthesis *in vivo*. A) Cysteine treatment increased intracellular RSS levels of wt and *Δsqr*. B) Both *Δsqr* and *Δcys11* lost the ability of growing in cysteine-deficient medium. C) Analysis of intracellular RSS levels of the wt, *Δcys11*, and *Δcys11Δsqr* strains. D) The *Δcys11* strain released more H_2S out than did the wt strain. E) MtDNA analysis of the wt, *Δcys11*, and cysteine treated *Δcys11* strains, 500 μM cysteine was used to treat *Δcys11*. F) *Δcys11* cells quickly precipitated down in 2 min, whereas wt cells did not precipitate. Data were from three independent experiments and presented as average ± SD. T-tests were performed to calculate the p-values, and asterisks indicate statistically significant difference (*p < 0.05, **p < 0.01, ***p < 0.001).

3.3. Mitochondrial integrity and functionality were damaged by sqr knock-out

Although both wt and *Δsqr* showed reduced growth in a non-fermentable medium (with glycerol or galactose as the main carbon source) compared to in a fermentable medium (with glucose as the main carbon source), *Δsqr* had a more obvious growth reduction (Fig. 3A), suggesting that mitochondria may be impaired in *Δsqr* cells. To observe the mitochondrial morphology *in vivo*, a GFP was fused with a leading peptide to localize it into mitochondrial inner membrane. The fused GFP was expressed in both wt and *Δsqr*. Laser confocal microscopic observation revealed that mitochondria in wt had regular rod shape; whereas, those in *Δsqr* were mostly fragmentized and scattered (Fig. 3B).

We also checked other characteristics of mitochondria. The relative number of mtDNA (mitochondrial DNA normalized against nuclear DNA), mitochondrial membrane potentials, and oxygen consumption rates were all lower in *Δsqr* than in wt (Fig. 3C–E). A higher level of intracellular ROS (reactive oxygen species) was detected in *Δsqr* compared to that of wt (Fig. 3F). The above results demonstrated that mitochondria health was impaired in the *Δsqr* cells.

For confirmation, we also performed complementation experiments. The complementation strain (*Δsqr::sqr*) was constructed via integrating a *sqr* gene (with its native promoter) into the leu-32 site of *Δsqr* chromosome (Table S1). The growth, content of intracellular RSS, and mtDNA of the complementation strain were analyzed. Results showed that compared with *Δsqr*, *Δsqr::sqr* largely recovered these phenotypes (Fig. S1). Thus, it is highly expected that other phenotypes such as mitochondrial membrane potentials and oxygen consumption might also to be complemented. These assays and analysis confirmed that the abnormal phenotypes were caused by *sqr* deletion.

Except for the experiments conducted under normoxic condition, we also compared wt and *Δsqr* under hypoxic condition (Fig. S2). Results showed that both wt and *Δsqr* grew poorly (maximum OD_{600} was around 2.3, whereas under normoxic condition, it reached 8.0). As under normoxic condition, the mtDNA of *Δsqr* was significantly lower than that of wt. We compared the intracellular ROS levels of wt and *Δsqr* under normoxic and hypoxic conditions. Under hypoxia condition, ROS level was increased in both wt and *Δsqr*, and *Δsqr* had a higher increase compared to wt. The results suggested that SQR may have antioxidation function under hypoxia condition.

3.4. Cysteine treatment complemented sqr knock-out

The *Δsqr* strain totally lost the growth in a basic medium (SD or EMM) (Fig. 4A and B). The addition of RSS compounds including S_8, MeSSSMe, HS_nH, or the 3-Mst substrate 3-mercaptopyruvate (3-MP) into EMM medium did not restore the growth (Fig. 4B). $Na_2S_2O_3$ partially restored the growth. Interestingly, the addition of cysteine or glutathione significantly restored the growth. Cell viability analysis indicated that viability of the *Δsqr* cells was obviously increased by cysteine (Fig. 4C). Cell cycle analysis indicated that most *Δsqr* cells (91.5%) halted at G2 phage before cysteine treatment, and changed to 37.1% G1 cells, 57.0% G2 cells after 24 h of cysteine treatment (Fig. 4D). MtDNA number, mitochondrial membrane potential, and oxygen consumption rate were all increased in *Δsqr* cells after cysteine treatment (Fig. 4E–G). Laser confocal microscopic images demonstrated that the morphology of mitochondria returned to rod shape from dotted shape after cysteine treatment (Fig. 4H).

3.5. Cysteine synthase knock-out led to similar phenotypes as sqr knock-out

We checked intracellular RSS levels in wt and *Δsqr* before and after cysteine treatment and found that their RSS levels were significantly increased after cysteine treatment (Fig. 5A). We then constructed a cysteine synthase (Cys11) deletion strain *Δcys11*. As *Δsqr*, it lost the ability of growing in a cysteine-deficient medium (Fig. 5B). The *Δcys11* strain also contained lower level of intracellular RSS compared to wt when growing in YES medium (Fig. 5C). More H_2S was released out from the culture (Fig. 5D) of *Δcys11* than that of wt. Its mtDNA number was dramatically decreased and cysteine treatment restored the mtDNA number back (Fig. 5E). Its cells formed aggregates that easily precipitated down (Fig. 5F). These phenomena demonstrated that *Δcys11* had similar phenotypes as *Δsqr*.

To confirm the phenotype changes were caused by *cys11* deletion, we performed complementation experiments. The complementation strain (*Δcys11::cys11*) was constructed via integrating a *cys11* gene (with its native promoter) into the leu-32 site of *Δcys11* (Table S1). The growth, content of intracellular RSS, and mitochondrial copy number of the

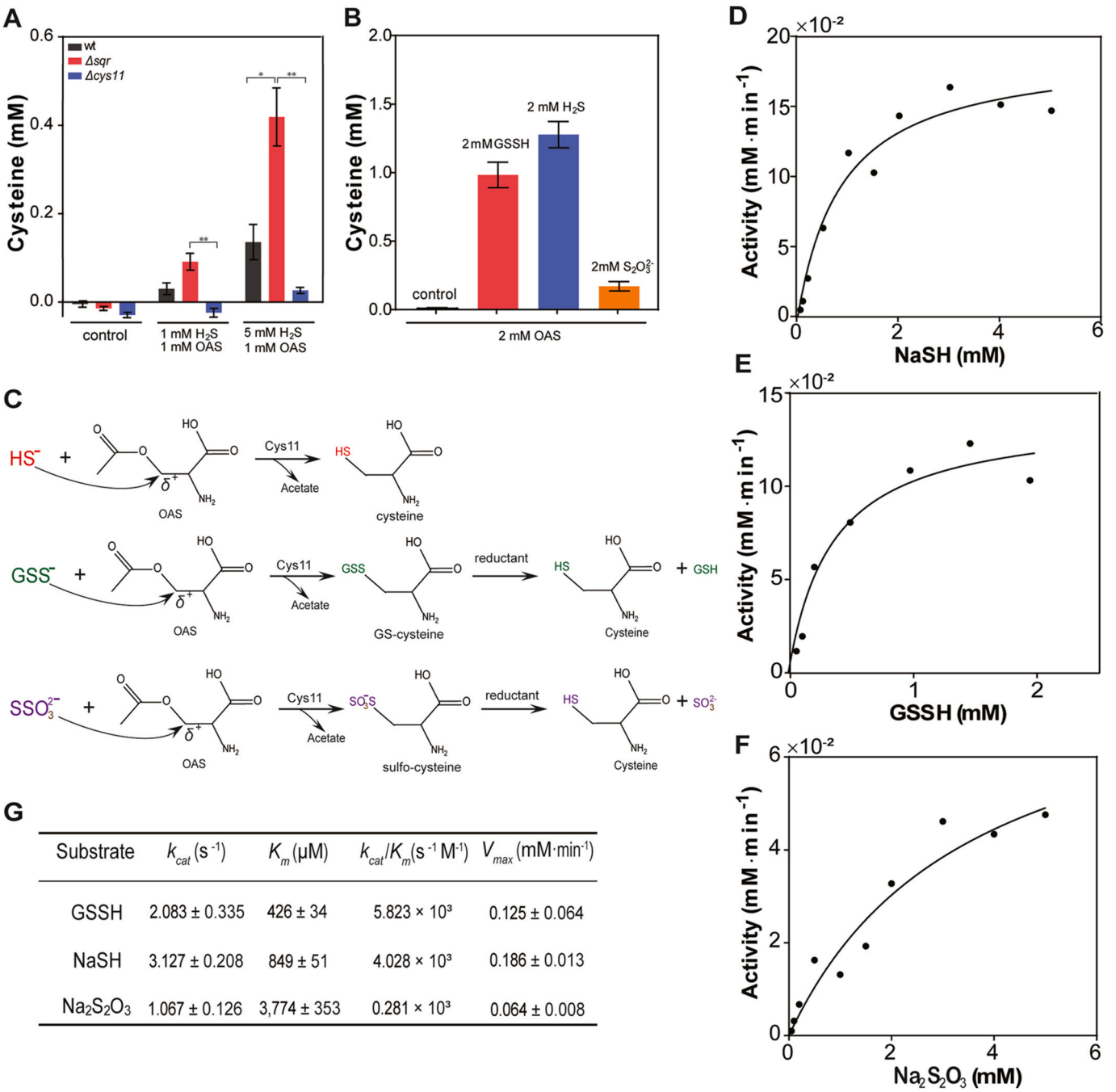

G

Substrate	k_{cat} (s^{-1})	K_m (μM)	k_{cat}/K_m ($s^{-1}M^{-1}$)	V_{max} ($mM \cdot min^{-1}$)
GSSH	2.083 ± 0.335	426 ± 34	5.823×10^3	0.125 ± 0.064
NaSH	3.127 ± 0.208	849 ± 51	4.028×10^3	0.186 ± 0.013
$Na_2S_2O_3$	1.067 ± 0.126	3,774 ± 353	0.281×10^3	0.064 ± 0.008

Fig. 6. *In vitro* examination of cysteine production. A) Cell lysates obtained from wt, *Δsqr*, and *Δcys11* were used for the reactions. Cysteine production was detected from wt and *Δsqr* cell lysates but not from that of *Δcys11*. B) Purified Cys11 was used for the reaction. Cysteine production was detected when using GSSH, H_2S, or thiosulfate as the substrate. C) The mechanisms of cysteine biosynthesis from H_2S, GSSH, and thiosulfate. D-G) Kinetic assays of Cys11 with different substrates. Data were from three independent experiments and presented as average ± SD. T-tests were performed to calculate the p-values, and asterisks indicate statistically significant difference (*$p < 0.05$, **$p < 0.01$).

complementation strain were analyzed. Results showed that compared with *Δcys11*, *Δcys11::cys11* largely recovered these phenotypes (Fig. S1). Thus, it is expected that other phenotypes might also to be complemented. These analysis confirmed that the abnormal phenotypes were caused by *cys11* deletion.

A *ΔsqrΔcys11* double knock-out strain was constructed and it contained even less intracellular RSS than *Δcys11* or *Δsqr* (Fig. 5C). These observations indicated that cysteine was converted into RSS *in vivo*.

3.6. Sqr knock-out blocked cysteine biosynthesis at the substrate level

We extracted cell lysates containing Cys11 from the wt, *Δsqr* and *Δcys11* strains, and then added H_2S and O-acetyl-L-serine (OAS), which are two reported substrates of cysteine synthase in many eukaryotic and prokaryotic cells, into the extracted cell lysates. Cysteine production was detected from both wt and *Δsqr* cell lysates but not from that of *Δcys11* (Fig. 6A), suggesting that Cys11 is expressed and functional in *Δsqr* as well as in wt. Since the *Δsqr* strain produced more H_2S and less RSS than did wt strain, we suspected that Cys11 may not use H_2S for cysteine biosynthesis *in vivo*. Instead, it might use RSS as its substrate. To test this

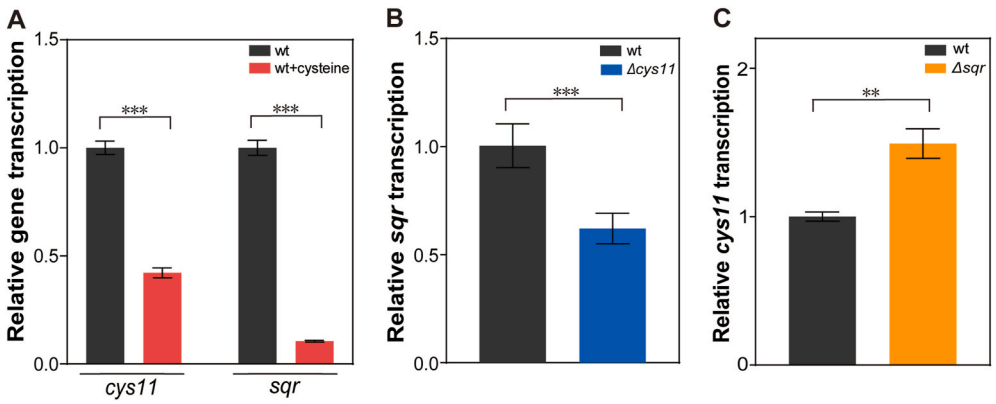

Fig. 7. Analysis of *cys11* and *sqr* expression with qRT-PCR. A) Cysteine treatment (500 μM) decreased the transcription level of both *cys11* and *sqr* in wt. B) Transcription of *sqr* was lower in *Δcys11* than in wt. C) Transcription of *cys11* was higher in *Δsqr* than in wt. Data were from three independent experiments and presented as average ± SD. T-tests were performed to calculate the p-values, and asterisks indicate statistically significant difference (**p < 0.01, ***p < 0.001).

possibility, we cloned Cys11 with a MBP (maltose binding protein)-tag at N-terminus, expressed it in *E. coli* BL21(DE3), and purified the recombinant protein by using amylose resin. The purified Cys11 used OAS and H_2S or GSSH to produce cysteine (Fig, 6B). Since $Na_2S_2O_3$ partially restored the growth of *Δsqr* in EMM medium, we tested it as well and found that Cys11 used $Na_2S_2O_3$ as a low efficient substrate for cysteine biosynthesis too. These results indicated that RSS can be used as an alternative substrate of Cys11 for cysteine synthesis.

When using GSSH or $Na_2S_2O_3$ as the substrate of Cys11, an intermediate compound should be formed (Fig. 6C). For confirmation, we used LC-MS to analyze the products. The GS-cysteine and sulfo-cysteine intermediates were both detected by LC-MS (Figure S3, A-C). Since the intermediates contain a disulfide bond, we added a reductant tris-(2-carboxyethyl)-phosphine (TCEP) to break this bond. LC-MS analysis indicated that after TCEP treatment, the content of GS-cysteine was sharply decreased and cysteine production was detected (Figure S3, D-E). We also observed that the production of GS-cysteine was much higher than that of sulfo-cysteine in the same experimental conditions (Figs. S3 and E), indicating that for Cys11, GSSH is a more efficient substrate than $Na_2S_2O_3$.

For further confirmation, we performed MS^2 analysis on the enzymatic products. The GS-cysteine MS^2 profile was consistent as predicted (Figs. S4 and A). After TCEP treatment, the suspected cysteine product was analyzed and its MS^2 profile was consistent with that of authentic cysteine (Figs. S4 and B). The MS^2 profile of sulfo-cysteine was also consistent with that of authentic compound (Figs. S4 and C). These results confirmed that the conclusions obtained from MS^1 results were correct.

We then assayed the kinetics of Cys11 with different substrates (Fig. 6D–G). The K_m value of GSSH was the lowest. The K_m values of H_2S (NaSH) and $Na_2S_2O_3$ were 2-fold and 9-fold higher than that of GSSH, respectively. Other kinetic parameters including k_{cat}, k_{cat}/K_m, and V_{max} were also calculated. GSSH and H_2S showed apparent advantages over $Na_2S_2O_3$ according to these kinetic parameters.

3.7. Expression of sqr and Cys11 were intertwined

We examined transcription levels of *sqr* and *cys11* in wt by using the quantitative reverse transcription PCR (qRT-PCR) method. When wt cells were treated with cysteine, the transcriptional levels of *sqr* and *cys11* both decreased (Fig. 7A). In addition, *sqr* showed an obviously lower transcription level in *Δcys11* than that in wt (Fig. 7B), while *cys11* had a higher transcriptional level in *Δsqr* than that in wt (Fig. 7C). These results suggested that the expression of both genes were inhibited when cysteine was abundant, and *cys11* expression was stimulated by Sqr knock-out due to lack of cysteine but *sqr* expression was not stimulated by Cys11 knock-out.

3.8. Systematically investigation of the transcription and metabolism changes caused by sqr knock-out

Transcriptomics and metabolomics were analyzed with wt and *Δsqr*. Both strains were cultivated in YES medium for 12 h, and then transferred into EMM medium for 12-h additional incubation before cells were collected. Through transcriptomic analysis, we found that 759 genes were upregulated and 584 genes were downregulated (fold change >2, p < 0.05) in *Δsqr* referred to those in wt (Fig. 8A). The percentage of transcription-changed genes was about 26% of the whole genome, reflecting a wide change caused by Sqr knock-out. KEGG pathways enrichment indicated that many metabolic pathways were influenced (Figs. S5 and S6.), such as pathways of organic acids, arginine, and lysine biosynthesis were upregulated; pathways of steroid and fatty acid biosynthesis were downregulated. Most genes involved in the transport and metabolism of cysteine were upregulated in *Δsqr* (Fig. 8B). Some genes critical for apoptosis were upregulated in *Δsqr* (Fig. 8C). The genes involved in cell cycle regulation were transcriptionally altered (Fig. 8D), which may explain the abnormal cell cycle of *Δsqr* cells.

We targeted 200 metabolites of central and energetic metabolism (supplementary information, sheet 1) in metabolome analysis. Among them, 133 compounds were identified with 100 showing significant change between *Δsqr* and wt (fold change >1.5, p < 0.05) (Fig. 9A). For specification:

I) The concentrations of both NADH and NAD^+ were dramatically decreased in *Δsqr* with *Δsqr*/wt ratios of 0.11 and 0.14 for NADH and NAD^+, respectively (Fig. S7). The concentration of flavin mononucleotide (FMN) was increased in *Δsqr* with a *Δsqr*/wt ratio of 1.89.
II) L-serine, the precursor for L-cysteine was accumulated in *Δsqr* strain (Fig. 9B), reflected by a *Δsqr*/wt ratio of 2.91.
III) Some metabolites of TCA cycle were obviously changed (Fig. 9B), including malate (*Δsqr*/wt ratio of 2.63), citrate (*Δsqr*/wt ratio of 2.16), succinate (*Δsqr*/wt ratio of 6.50), fumarate (*Δsqr*/wt ratio of 2.32), andcis-aconitic acid (*Δsqr*/wt ratio of 0.10)

Overall, these results indicated that the cysteine biosynthesis, the respiration chain and TCA cycle were dramatically changed by Sqr knock-out.

4. Discussion

H_2S has been deemed as the third gaseous signal after NO and CO in mammals [33–35]. Recently, more and more studies indicated that H_2S may function via forming RSS [36,37]. This necessitates the study of Sqr function in eukaryotic cells. In this work, we verified that Sqr is a more

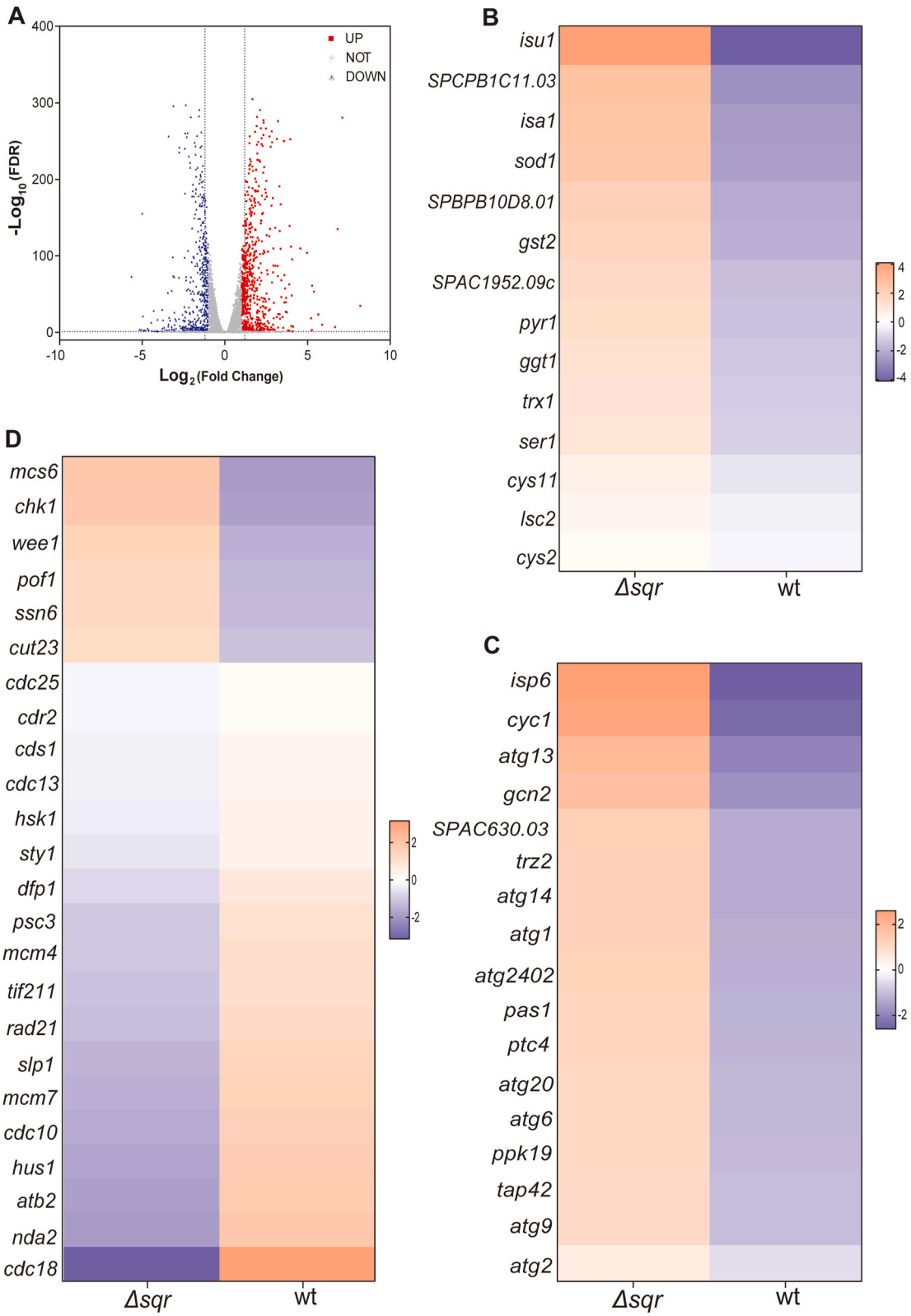

Fig. 8. Transcriptome analysis of the wt and *Δsqr* strains. A) Numbers of upregulated, downregulated, and not changed genes. B-D) Specific genes that were changed at transcriptional level. The analysis was performed with three parallel biological samples.

important RSS producer than 3-Mst for mitochondria (Fig. 10A). Its knock-out led to wide changes in transcriptome and metabolome profiles. Mitochondria health is heavily dependent on Sqr, evidenced by the abnormal morphology and function of mitochondria in Sqr knock-out strain.

We also found that Sqr is required for cysteine synthesis in *S. pombe*. This strain contains no Cbs or Cse, hence cannot convert methionine to cysteine. The *de novo* biosynthesis pathway is the only route for cysteine production in it. H_2S has been deemed as the substrate for *de novo* biosynthesis of cysteine in most eukaryotic and prokaryotic cells

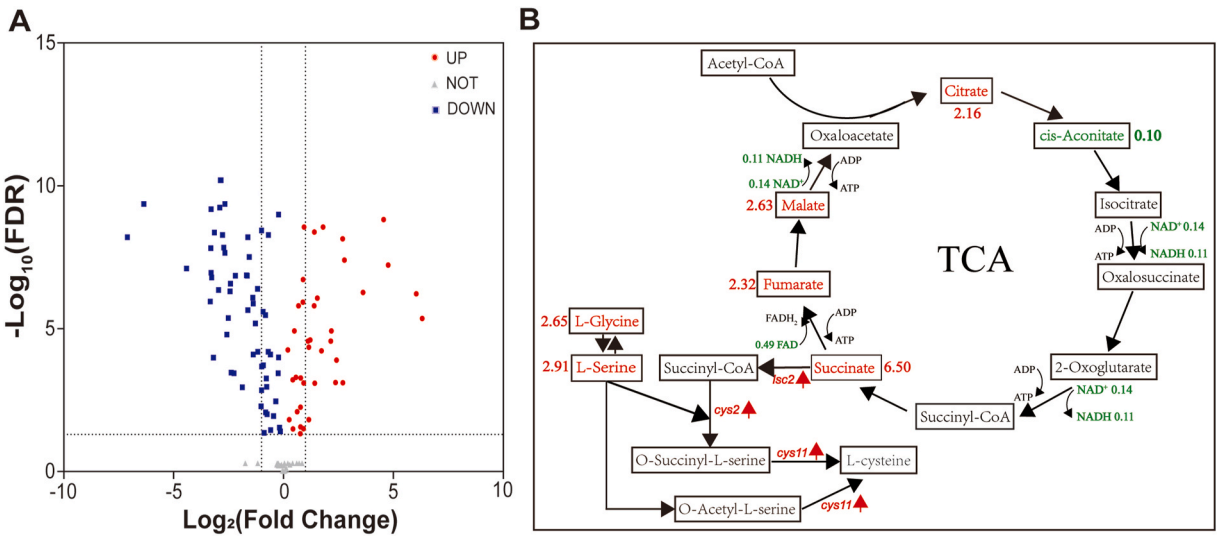

Fig. 9. Targeted metabolome analysis of wt and *Δsqr* strains. A) Numbers of upregulated, downregulated, and not changed metabolites. B) TCA cycle metabolites that showed different abundance in wt and *Δsqr*. Red color represents the metabolite is more abundant in *Δsqr* compared to wt, and green color represents the metabolite is less abundant in *Δsqr* compared to wt. The number represents the ratio of certain metabolite in the strains (*Δsqr*/wt). Arrows indicate the genes upregulated in *Δsqr* compared to wt. The analysis was performed with six parallel biological samples. (For interpretation of the references to color in this figure legend, the reader is referred to the Web version of this article.)

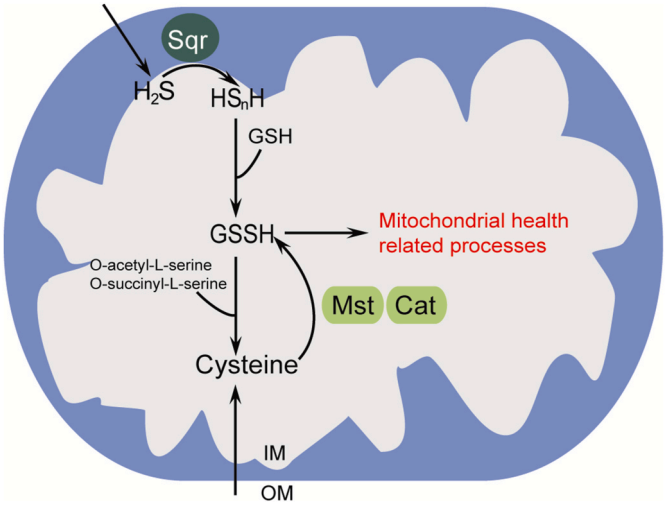

Fig. 10. Schematic representation of the relations among RSS production, cysteine biosynthesis, and mitochondrial health in *S. pombe*.

[38–40]. Thiosulfate can be used as the alternative substrate by cysteine synthase in some bacteria [41,42]. However, RSS involvement in cysteine *de novo* biosynthesis has not been reported previously. Herein, we suggested that RSS was the *de facto* substrate for cysteine biosynthesis *in vivo* based on lines of evidence. First, the *Δsqr* strain produced more H_2S but less RSS than wt strain, meanwhile it displayed a cysteine-deficient phenotype. Second, *in vitro* experiments demonstrated that RSS can be used as the substrate for Cys11-catalyzed cysteine synthesis. Cys11 showed lower K_m toward GSSH compared to H_2S. Third, the intracellular RSS is around 100 μM–400 μM; whereas, H_2S is 15 μM–50 μM. Other studies reported that intracellular H_2S is even low to 10 nM–30 nM quantified with different methods [27,43,44]. Fourth, RSS is more stable than H_2S in the cell [45], the latter easily releases out as gas; therefore, RSS provides a relatively constant substrate reservoir for Cys11.

RSS is a more reactive substrate than H_2S. Previous studies have revealed that RSS, for instance, glutathione persulfide (GSSH) and cysteine persulfide (CysSSH), have lower pK_a values than H_2S, and GSSH and CysSSH are more nucleophilic than H_2S [45,46]. OAS and O-succinyl-L-serine (OSS) are two precursors of cysteine in *S. pombe* [47]. The reaction between H_2S/GSSH/$S_2O_3^{2-}$ and OAS/OSS is initiated by the nucleophilic attack of H_2S/GSSH/$S_2O_3^{2-}$ toward the electrophilic carbon atom in OAS/OSS. Hence, compared to H_2S and $S_2O_3^{2-}$, the more nucleophilic GSSH is more reactive for this reaction (Fig. 6C). Except for GSSH, there are other RSS present in the cell, such as Cys-SSH, CoASSH, and HS_nH. Herein we only tested two species (GSSH and thiosulfate) because they are easily prepared and more importantly, they contain very low or zero amount of HS^-. In contrast, chemically prepared HS_nH (by mixing S_8 and NaSH) often contains high amount of HS^-, which will introduce a disturbance factor into experiments. However, chemically analysis indicate that HS_nH is more active than RSSH, and hence HS_nH may also involves in cysteine biosynthesis in the cell.

Adding RSS compounds directly into medium cannot restore the growth of *Δsqr*, suggesting that the import of RSS into mitochondria is difficult. This was consistent with our previous findings that treating yeast cells with RSS cannot obviously increase their intracellular RSS level; whereas, cysteine or cystine can [48]. 3-Mst, together with cysteine aminotransferase (CAT), can convert transported cysteine to RSS in *S. pombe*, which explains the increase of intracellular RSS after cysteine treatment. Thiosulfate partially restored the growth of *Δsqr*, probably because thiosulfate can be converted to RSS by rhodaneses like 3-Mst in cytoplasm or mitochondria, other than being used as the direct substrate of Cys11 because its K_m is too low.

We also observed that ROS level was increased in *Δsqr*; therefore, in addition to cysteine biosynthesis, RSS should be involved in other biological processes that are important for mitochondrial health, which deserves further investigations. Combining all the results, we proposed that Sqr, mitochondrial health, and cysteine biosynthesis are interwound in *S. pombe*. First, the Sqr-catalyzed H_2S oxidation and 3-Mst (and other rhodaneses)-catalyzed cysteine conversion to RSS are two resources of intracellular RSS. When exogenous cysteine nutrient is lacking, the former becomes the main RSS resource. Second, RSS is the *de facto* substrate for cysteine biosynthesis other than H_2S. Sqr knock-out results in RSS shortage, thereby leading to cysteine deficiency. Third, both RSS and cysteine are important for maintaining mitochondrial health. However, cysteine functions at least partially via forming RSS (Fig. 10).

In conclusion, our study has three important findings:

I) Sqr is an important RSS producer in mitochondria in *S. pombe*. It plays a more critical role than 3-Mst in respect of mitochondrial RSS generation.
II) RSS is involved in cysteine *de novo* biosynthesis. It is the *de facto* substrate of cysteine synthase in S. pombe.
III) Sqr is required for maintaining the health of mitochondria. Its knock-out leads RSS shortage, functional deficiency of mitochondria, and early apoptosis of cells. Thus, Sqr might be a new target for inhibiting cell proliferation.

Author contributions

H. Liu and L. Xun designed the research and made plans for the experiments; X. Zhang and Y. Xin performed the experiments; Z. Chen helped in S. pombe mutant construction; Y. Xia helped in data interpretation.

Data availability

The omics data have been deposited in https://www.biosino.org/node/with ID: OEP002326. Others are available from the corresponding author upon reasonable request.

Declaration of competing interest

The authors declare that they have no known competing financial interests or personal relationships that could have appeared to influence the work reported in this paper.

Acknowledgements

The work was financially supported by grants from the National Key R&D Program of China (2018YFA0901200), and the National Natural Science Foundation of China (91951202). The authors also thank the support from State Key Laboratory of Microbial Technology, Shandong University.

Appendix A. Supplementary data

Supplementary data to this article can be found online at https://doi.org/10.1016/j.redox.2021.102169.

References

[1] S. Papa, Mitochondrial oxidative phosphorylation changes in the life span. Molecular aspects and physiopathological implications, Biochim. Biophys. Acta 1276 (1996) 87–105, https://doi.org/10.1016/0005-2728(96)00077-1.
[2] J.B. Spinelli, M.C. Haigis, The multifaceted contributions of mitochondria to cellular metabolism, Nat. Cell Biol. 20 (2018) 745–754, https://doi.org/10.1038/s41556-018-0124-1.
[3] K. Palikaras, E. Lionaki, N. Tavernarakis, Mechanisms of mitophagy in cellular homeostasis, physiology and pathology, Nat. Cell Biol. 20 (2018) 1013–1022, https://doi.org/10.1038/s41556-018-0176-2.
[4] J.R. Friedman, J. Nunnari, Mitochondrial form and function, Nature 505 (2014) 335–343, https://doi.org/10.1038/nature12985.
[5] B. Van Houten, S.E. Hunter, J.N. Meyer, Mitochondrial DNA damage induced autophagy, cell death, and disease, Front. Biosci. - Landmark. 21 (2016) 42–54, https://doi.org/10.2741/4375.
[6] J. O'Malley, R. Kumar, J. Inigo, N. Yadava, D. Chandra, Mitochondrial stress response and cancer, Trends in Cancer 6 (2020) 688–701, https://doi.org/10.1016/j.trecan.2020.04.009.
[7] H. Liu, M.N. Radford, C. tao Yang, W. Chen, M. Xian, Inorganic hydrogen polysulfides: chemistry, chemical biology and detection, Br. J. Pharmacol. 176 (2019) 616–627, https://doi.org/10.1111/bph.14330.
[8] J.M. Fukuto, L.J. Ignarro, P. Nagy, D.A. Wink, C.G. Kevil, M. Feelisch, M. M. Cortese-Krott, C.L. Bianco, Y. Kumagai, A.J. Hobbs, J. Lin, T. Ida, T. Akaike, Biological hydropersulfides and related polysulfides – a new concept and perspective in redox biology, FEBS Lett. 592 (2018) 2140–2152, https://doi.org/10.1002/1873-3468.13090.
[9] M. Iciek, A. Bilska-Wilkosz, M. Górny, Sulfane sulfur - new findings on an old topic, Acta Biochim. Pol. 66 (2019) 533–544, https://doi.org/10.18388/abp.2019_2909.
[10] N. Lau, M.D. Pluth, Reactive sulfur species (RSS): persulfides, polysulfides, potential, and problems, Curr. Opin. Chem. Biol. 49 (2019) 1–8, https://doi.org/10.1016/j.cbpa.2018.08.012.
[11] T. Zhang, H. Tsutsuki, K. Ono, T. Akaike, T. Sawa, Antioxidative and anti-inflammatory actions of reactive cysteine persulfides, J. Clin. Biochem. Nutr. 68 (2021) 5–8, https://doi.org/10.3164/jcbn.20-13.
[12] T.V. Mishanina, M. Libiad, R. Banerjee, Biogenesis of reactive sulfur species for signaling by hydrogen sulfide oxidation pathways, Nat. Chem. Biol. 11 (2015) 457–464, https://doi.org/10.1038/nchembio.1834.
[13] Y. Xia, C. Lü, N. Hou, Y. Xin, J. Liu, H. Liu, L. Xun, Sulfide production and oxidation by heterotrophic bacteria under aerobic conditions, ISME J. 11 (2017) 2754–2766, https://doi.org/10.1038/ismej.2017.125.
[14] M. Goubern, M. Andriamihaja, T. Nübel, F. Blachier, F. Bouillaud, Sulfide, the first inorganic substrate for human cells, FASEB J. Off. Publ. Fed. Am. Soc. Exp. Biol. 21 (2007) 1699–1706, https://doi.org/10.1096/fj.06-7407com.
[15] K.R. Olson, Mitochondrial adaptations to utilize hydrogen sulfide for energy and signaling, J. Comp. Physiol. B Biochem. Syst. Environ. Physiol. 182 (2012) 881–897, https://doi.org/10.1007/s00360-012-0654-y.
[16] V. Vitvitsky, O. Kabil, R. Banerjee, High turnover rates for hydrogen sulfide allow for rapid regulation of its tissue concentrations, Antioxidants Redox Signal. 17 (2012) 22–31, https://doi.org/10.1089/ars.2011.4310.
[17] V. Tiranti, P. D'Adamo, E. Briem, G. Ferrari, R. Mineri, E. Lamantea, H. Mandel, P. Balestri, M.-T. Garcia-Silva, B. Vollmer, P. Rinaldo, S.H. Hahn, J. Leonard, S. Rahman, C. Dionisi-Vici, B. Garavaglia, P. Gasparini, M. Zeviani, Ethylmalonic encephalopathy is caused by mutations in ETHE1, a gene encoding a mitochondrial matrix protein, Am. J. Hum. Genet. 74 (2004) 239–252, https://doi.org/10.1086/381653.
[18] T. Akaike, T. Ida, F.Y. Wei, M. Nishida, Y. Kumagai, M.M. Alam, H. Ihara, T. Sawa, T. Matsunaga, S. Kasamatsu, A. Nishimura, M. Morita, K. Tomizawa, A. Nishimura, S. Watanabe, K. Inaba, H. Shima, N. Tanuma, M. Jung, S. Fujii, Y. Watanabe, M. Ohmuraya, P. Nagy, M. Feelisch, J.M. Fukuto, H. Motohashi, Cysteinyl-tRNA synthetase governs cysteine polysulfidation and mitochondrial bioenergetics, Nat. Commun. 8 (2017), https://doi.org/10.1038/s41467-017-01311-y.
[19] F. Bouillaud, F. Blachier, Mitochondria and sulfide: a very old story of poisoning, feeding, and signaling? Antioxidants Redox Signal. 15 (2011) 379—391, https://doi.org/10.1089/ars.2010.3678.
[20] C.S. Hoffman, V. Wood, P.A. Fantes, An ancient yeast for young geneticists: a primer on the Schizosaccharomyces pombe model system, Genetics 201 (2015) 403–423, https://doi.org/10.1534/genetics.115.181503.
[21] Y. Zhao, H.B. Lieberman, Schizosaccharomyces pombe: a model for molecular studies of eukaryotic genes, DNA Cell Biol. 14 (1995) 359–371, https://doi.org/10.1089/dna.1995.14.359.
[22] V. Wood, R. Gwilliam, M.-A. Rajandream, M. Lyne, R. Lyne, A. Stewart, J. Sgouros, N. Peat, J. Hayles, S. Baker, D. Basham, S. Bowman, K. Brooks, D. Brown, S. Brown, T. Chillingworth, C. Churcher, M. Collins, R. Connor, A. Cronin, P. Davis, T. Feltwell, A. Fraser, S. Gentles, A. Goble, N. Hamlin, D. Harris, J. Hidalgo, G. Hodgson, S. Holroyd, T. Hornsby, S. Howarth, E.J. Huckle, S. Hunt, K. Jagels, K. James, L. Jones, M. Jones, S. Leather, S. McDonald, J. McLean, P. Mooney, S. Moule, K. Mungall, L. Murphy, D. Niblett, C. Odell, K. Oliver, S. O'Neil, D. Pearson, M.A. Quail, E. Rabbinowitsch, K. Rutherford, S. Rutter, D. Saunders, K. Seeger, S. Sharp, J. Skelton, M. Simmonds, R. Squares, S. Squares, K. Stevens, K. Taylor, R.G. Taylor, A. Tivey, S. Walsh, T. Warren, S. Whitehead, J. Woodward, G. Volckaert, R. Aert, J. Robben, B. Grymonprez, I. Weltjens, E. Vanstreels, M. Rieger, M. Schäfer, S. Müller-Auer, C. Gabel, M. Fuchs, A. Düsterhöft, C. Fritzc, E. Holzer, D. Moestl, H. Hilbert, K. Borzym, I. Langer, A. Beck, H. Lehrach, R. Reinhardt, T.M. Pohl, P. Eger, W. Zimmermann, H. Wedler, R. Wambutt, B. Purnelle, A. Goffeau, E. Cadieu, S. Dréano, S. Gloux, V. Lelaure, S. Mottier, F. Galibert, S.J. Aves, Z. Xiang, C. Hunt, K. Moore, S.M. Hurst, M. Lucas, M. Rochet, C. Gaillardin, V.A. Tallada, A. Garzon, G. Thode, R.R. Daga, L. Cruzado, J. Jimenez, M. Sánchez, F. del Rey, J. Benito, A. Domínguez, J.L. Revuelta, S. Moreno, J. Armstrong, S.L. Forsburg, L. Cerutti, T. Lowe, W.R. McCombie, I. Paulsen, J. Potashkin, G. V Shpakovski, D. Ussery, B.G. Barrell, P. Nurse, The genome sequence of Schizosaccharomyces pombe, Nature 415 (2002) 871–880, https://doi.org/10.1038/nature724.
[23] J.L. Luebke, J. Shen, K.E. Bruce, T.E. Kehl-Fie, H. Peng, E.P. Skaar, D.P. Giedroc, The CsoR-like sulfurtransferase repressor (CstR) is a persulfide sensor in Staphylococcus aureus, Mol. Microbiol. 94 (2014) 1343–1360, https://doi.org/10.1111/mmi.12835.
[24] H. Liu, Y. Xin, L. Xun, Distribution, diversity, and activities of sulfur dioxygenases in heterotrophic bacteria, Appl. Environ. Microbiol. 80 (2014) 1799–1806, https://doi.org/10.1128/AEM.03281-13.
[25] A.J. Kamyshny, A. Goifman, J. Gun, D. Rizkov, O. Lev, Equilibrium distribution of polysulfide ions in aqueous solutions at 25 degrees C: a new approach for the study of polysulfides' equilibria, Environ. Sci. Technol. 38 (2004) 6633–6644, https://doi.org/10.1021/es049514e.
[26] Y. Xin, H. Liu, F. Cui, H. Liu, L. Xun, Recombinant Escherichia coli with sulfide: quinone oxidoreductase and persulfide dioxygenase rapidly oxidises sulfide to sulfite and thiosulfate via a new pathway, Environ. Microbiol. 18 (2016) 5123–5136, https://doi.org/10.1111/1462-2920.13511.
[27] M. Ran, T. Wang, M. Shao, Z. Chen, H. Liu, Y. Xia, L. Xun, Sensitive method for reliable quantification of sulfane sulfur in biological samples, Anal. Chem. 91 (2019), https://doi.org/10.1021/acs.analchem.9b02875.
[28] N.M. Kredich, G.M. Tomkins, The enzymic synthesis of L-cysteine in Escherichia coli and Salmonella typhimurium, J. Biol. Chem. 241 (1966) 4955–4965.

[29] G.K. Kolluru, X. Shen, S.C. Bir, C.G. Kevil, Hydrogen sulfide chemical biology: pathophysiological roles and detection, Nitric Oxide Biol. Chem. 35 (2013) 5–20, https://doi.org/10.1016/j.niox.2013.07.002.
[30] F. Madeo, E. Fröhlich, K.U. Fröhlich, A yeast mutant showing diagnostic markers of early and late apoptosis, J. Cell Biol. 139 (1997) 729–734, https://doi.org/10.1083/jcb.139.3.729.
[31] E. Herker, H. Jungwirth, K.A. Lehmann, C. Maldener, K.-U. Fröhlich, S. Wissing, S. Büttner, M. Fehr, S. Sigrist, F. Madeo, Chronological aging leads to apoptosis in yeast, J. Cell Biol. 164 (2004) 501–507, https://doi.org/10.1083/jcb.200310014.
[32] S.B. Haase, D.J. Lew, Flow cytometric analysis of DNA content in budding yeast, Methods Enzymol. 283 (1997) 322–332, https://doi.org/10.1016/s0076-6879(97)83026-1.
[33] H. Kimura, Signalling by hydrogen sulfide and polysulfides via protein S-sulfuration, Br. J. Pharmacol. (2019), https://doi.org/10.1111/bph.14579.
[34] J. Shen, B.J.C. Walsh, A.L. Flores-Mireles, H. Peng, Y. Zhang, Y. Zhang, J. C. Trinidad, S.J. Hultgren, D.P. Giedroc, Hydrogen sulfide sensing through reactive sulfur species (RSS) and nitroxyl (HNO) in *Enterococcus faecalis*, ACS Chem. Biol. 13 (2018) 1610–1620, https://doi.org/10.1021/acschembio.8b00230.
[35] M.R. Filipovic, J. Zivanovic, B. Alvarez, R. Banerjee, Chemical biology of H(2)S signaling through persulfidation, Chem. Rev. 118 (2018) 1253–1337, https://doi.org/10.1021/acs.chemrev.7b00205.
[36] C.L. Bianco, T.A. Chavez, V. Sosa, S.S. Saund, Q.N.N. Nguyen, D.J. Tantillo, A. S. Ichimura, J.P. Toscano, J.M. Fukuto, The chemical biology of the persulfide (RSSH)/perthiyl (RSS·) redox couple and possible role in biological redox signaling, Free Radic. Biol. Med. 101 (2016) 20–31, https://doi.org/10.1016/j.freeradbiomed.2016.09.020.
[37] T. Ida, T. Sawa, H. Ihara, Y. Tsuchiya, Y. Watanabe, Y. Kumagai, M. Suematsu, H. Motohashi, S. Fujii, T. Matsunaga, M. Yamamoto, K. Ono, N.O. Devarie-Baez, M. Xian, J.M. Fukuto, T. Akaike, Reactive cysteine persulfides and S-polythiolation regulate oxidative stress and redox signaling, Proc. Natl. Acad. Sci. Unit. States Am. 111 (2014) 7606, https://doi.org/10.1073/pnas.1321232111. LP – 7611.
[38] K. Saito, Regulation of sulfate transport and synthesis of sulfur-containing amino acids, Curr. Opin. Plant Biol. 3 (2000) 188–195.
[39] V.D.B. Bonifácio, S.A. Pereira, J. Serpa, J.B. Vicente, Cysteine metabolic circuitries: druggable targets in cancer, Br. J. Cancer 124 (2021) 862–879, https://doi.org/10.1038/s41416-020-01156-1.
[40] Y. Kawano, K. Suzuki, I. Ohtsu, Current understanding of sulfur assimilation metabolism to biosynthesize L-cysteine and recent progress of its fermentative overproduction in microorganisms, Appl. Microbiol. Biotechnol. 102 (2018) 8203–8211, https://doi.org/10.1007/s00253-018-9246-4.
[41] T. Nakamura, H. Iwahashi, Y. Eguchi, Enzymatic proof for the identity of the S-sulfocysteine synthase and cysteine synthase B of Salmonella typhimurium, J. Bacteriol. 158 (1984) 1122–1127, https://doi.org/10.1128/jb.158.3.1122-1127.1984.
[42] G. Hensel, H.G. Trüper, O-Acetylserine sulfhydrylase and S-sulfocysteine synthase activities of *Rhodospirillum tenue*, Arch. Microbiol. 134 (1983) 227–232, https://doi.org/10.1007/BF00407763.
[43] K. Zhang, J. Meng, W. Bao, M. Liu, X. Wang, Z. Tian, Mitochondrion-targeting near-infrared fluorescent probe for detecting intracellular nanomolar level hydrogen sulfide with high recognition rate, Anal. Bioanal. Chem. 413 (2021) 1215–1224, https://doi.org/10.1007/s00216-020-03086-6.
[44] H. Kimura, Signaling molecules: hydrogen sulfide and polysulfide, Antioxidants Redox Signal. 22 (2015) 362–376, https://doi.org/10.1089/ars.2014.5869.
[45] K. Ono, T. Akaike, T. Sawa, Y. Kumagai, D.A. Wink, D.J. Tantillo, A.J. Hobbs, P. Nagy, M. Xian, J. Lin, J.M. Fukuto, Redox chemistry and chemical biology of H2S, hydropersulfides, and derived species: implications of their possible biological activity and utility, Free Radic. Biol. Med. 77 (2014) 82–94, https://doi.org/10.1016/j.freeradbiomed.2014.09.007.
[46] C.-M. Park, L. Weerasinghe, J.J. Day, J.M. Fukuto, M. Xian, Persulfides: current knowledge and challenges in chemistry and chemical biology, Mol. Biosyst. 11 (2015) 1775–1785, https://doi.org/10.1039/c5mb00216h.
[47] K. Bastard, A. Perret, A. Mariage, T. Bessonnet, A. Pinet-Turpault, J.-L. Petit, E. Darii, P. Bazire, C. Vergne-Vaxelaire, C. Brewee, A. Debard, V. Pellouin, M. Besnard-Gonnet, F. Artiguenave, C. Médigue, D. Vallenet, A. Danchin, A. Zaparucha, J. Weissenbach, M. Salanoubat, V. de Berardinis, Parallel evolution of non-homologous isofunctional enzymes in methionine biosynthesis, Nat. Chem. Biol. 13 (2017) 858–866, https://doi.org/10.1038/nchembio.2397.
[48] X. Hu, H. Li, X. Zhang, Z. Chen, R. Zhao, N. Hou, J. Liu, L. Xun, H. Liu, Developing polysulfide-sensitive GFPs for real-time analysis of polysulfides in live cells and subcellular organelles, Anal. Chem. 91 (2019) 3893–3901, https://doi.org/10.1021/acs.analchem.8b04634.